THE JOURNAL OF BIOLOGICAL CHEMISTRY VOL. 290, NO. 3, pp. 1364–1373, January 16, 2015

Site-directed Mutagenesis Switching a Dimethylallyl Tryptophan Synthase to a Specific Tyrosine C^3-Prenylating Enzyme*

Received for publication, November 4, 2014, and in revised form, November 26, 2014 Published, JBC Papers in Press, December 4, 2014, DOI 10.1074/jbc.M114.623413

Aili Fan (范爱丽)[‡1], Georg Zocher[§], Edyta Stec[‡], Thilo Stehle[§], and Shu-Ming Li (李书明)[‡2]

From the [‡]Institut für Pharmazeutische Biologie und Biotechnologie, Philipps-Universität Marburg, 35037 Marburg and the [§]Interfakultäres Institut für Biochemie, Eberhard Karls Universität Tübingen, 72076 Tübingen, Germany

Background: Dimethylallyl tryptophan synthase FgaPT2 catalyzes in nature the C^4-prenylation of indole ring.
Results: FgaPT2 also catalyzes *in vitro* a regular C^3-prenylation of L-tyrosine; its mutant FgaPT2_K174F showed a much higher catalytic activity toward L-tyrosine than L-tryptophan.
Conclusion: Single mutation on the key amino acid switches the tryptophan C^4-prenyltransferase to a tyrosine C^3-prenylating enzyme.
Significance: The first L-tyrosine C^3-prenylating enzyme was created by molecular modeling-guided mutagenesis.

The tryptophan prenyltransferases FgaPT2 and 7-DMATS (7-dimethylallyl tryptophan synthase) from *Aspergillus fumigatus* catalyze C^4- and C^7-prenylation of the indole ring, respectively. 7-DMATS was found to accept L-tyrosine as substrate as well and converted it to an *O*-prenylated derivative. An acceptance of L-tyrosine by FgaPT2 was also observed in this study. Interestingly, isolation and structure elucidation revealed the identification of a C^3-prenylated L-tyrosine as enzyme product. Molecular modeling and site-directed mutagenesis led to creation of a mutant FgaPT2_K174F, which showed much higher specificity toward L-tyrosine than L-tryptophan. Its catalytic efficiency toward L-tyrosine was found to be 4.9-fold in comparison with that of non-mutated FgaPT2, whereas the activity toward L-tryptophan was less than 0.4% of that of the wild-type. To the best of our knowledge, this is the first report on an enzymatic *C*-prenylation of L-tyrosine as free amino acid and altering the substrate preference of a prenyltransferase by mutagenesis.

Prenyltransferases catalyze the transfer reactions of prenyl moieties from different prenyl donors, *e.g.* dimethylallyl diphosphate (DMAPP),[3] to various aliphatic or aromatic acceptors and play an important role as modification enzymes for creating structural diversity of numerous natural products (1). Prenylated derivatives often show biological and pharmacological activities clearly distinct from their non-prenylated precursors (1–5), which make these enzymes valuable biocatalysts in the structural modification of small molecules. These features have drawn noteworthy attention of scientists from different disciplines (6–8).

According to their sequences, biochemical properties, and structures, prenyltransferases can be divided into several subgroups (1, 9, 10). One of the most investigated subgroups is the dimethylallyl tryptophan synthase (DMATS) superfamily from microorganisms. Until now, more than 40 such enzymes have been identified and characterized biochemically (8, 11–14). The majority of the DMATS superfamily is involved in the biosynthesis of prenylated indole alkaloids and takes indole derivatives including tryptophan and tryptophan-containing cyclic dipeptides as substrates (3, 8). Usually, they showed significant substrate tolerance toward different aromatic substrates, but catalyzed regiospecific Friedel-Crafts alkylations of the indole ring. These features make the DMATS prenyltransferases useful tools as biocatalysts for production of prenylated products (8). For example, FgaPT2 catalyzes the first pathway-specific step in the biosynthesis of the ergot alkaloid fumigaclavine C in *Aspergillus fumigatus*, *i.e.* a regular prenylation of L-tryptophan at position C-4 of the indole moiety in the presence of DMAPP (Fig. 1) (15, 16). It was later demonstrated that FgaPT2 also accepted DMAPP analogues as alkyl donors (17, 18) and accepted simple tryptophan derivatives (19), tryptophan-containing cyclic dipeptides (19), or even hydroxynaphthalenes (20) as acceptors. The crystal structure of FgaPT2 was determined in 2009 and used as basis for understanding the prenylation mechanism (21, 22). Another example of this superfamily, 7-DMATS, catalyzes a C^7-prenylation of L-tryptophan on the indole ring (23) and is involved in the biosynthesis of astechrome in *A. fumigatus* (24). FgaPT2 and 7-DMATS share a sequence identity of 31% on the amino acid level.

A few members of the DMATS superfamily catalyze prenylations of non-indole derivatives, and in some cases, *O*-prenylations (25, 26). One example of such enzymes, SirD from *Leptosphaeria maculans*, is involved in the biosynthesis of sirodesmin PL and responsible for the *O*-prenylation of the phenolic hydroxyl group in L-tyrosine (26, 27). SirD shares a sequence identity of 34% on the amino acid level with 7-DMATS and also accepts L-tryptophan and some of its derivatives as aromatic substrates. It catalyzes mainly a C^7-prenyla-

* This work was supported in part by Deutsche Forschungsgemeinschaft Grants Li844/4-1 (to S.-M. L.) and SFB766 (to G. Z. and T. S.).
[1] Recipient of a scholarship from the China Scholarship Council.
[2] To whom correspondence should be addressed. Tel.: 49-6421-2822461; Fax: 49-6421-2825365; E-mail: shuming.li@staff.uni-marburg.de.
[3] The abbreviations used are: DMAPP, dimethylallyl diphosphate; DMATS, dimethylallyl tryptophan synthase; DMSPP, dimethylallyl *S*-thiolodiphosphate; HSQC, heteronuclear single quantum correlation; HMBC, heteronuclear multiple bond correlation.

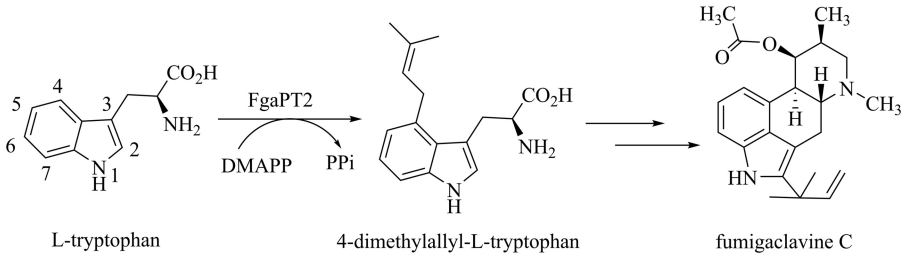

FIGURE 1. **Prenyl transfer reaction catalyzed by FgaPT2 in the biosynthesis of fumigaclavine C.**

tion of the indole ring (26, 28, 29). C^7-Prenylation of L-tryptophan by tyrosine prenyltransferases was also demonstrated recently with TyrPT from *Aspergillus niger* (14). Encouraged by the results obtained for SirD and TyrPT with L-tryptophan as substrate, we investigated the behavior of 7-DMATS from *A. fumigatus* toward L-tyrosine in the presence of DMAPP. 7-DMATS was also able to take L-tyrosine and two derivatives thereof as substrates and catalyzed the same *O*- or *N*-prenylation as the two tyrosine *O*-prenyltransferases SirD and TyrPT (14, 28–30). These results demonstrated the complementary substrate and catalytic promiscuity of tryptophan and tyrosine prenyltransferases and meanwhile raised the question about the acceptance of L-tyrosine and derivatives by other tryptophan prenyltransferases, such as FgaPT2, 5-DMATS, and 6-$DMATS_{Sa}$, which catalyze the L-tryptophan prenylation at C-4, C-5, and C-6, respectively (11, 15, 31). To gain more insights into the behavior of these enzymes toward tyrosine and derivatives, FgaPT2, 5-DMATS, and 6-$DMATS_{Sa}$ were overproduced and purified as described previously (11, 19, 31) and incubated with L-tyrosine at 37 °C for 16 h. Incubations with L-tryptophan were used as positive controls. The incubation mixtures were then analyzed on HPLC.

TABLE 1

Mutated derivatives of FgaPT2 and respective primers used for site-directed mutagenesis

Annealing temperatures for PCR varied from 55 to 65 °C, and elongation time was 7.5 min; bold letters in primers indicated mutation in comparison with the original sequence of FgaPT2.

Mutant	Primer	Sequence (5'-3')	Plasmid
FgaPT2_E89A	fw	GATACGGCACTCCGTTCG**C**ATTGAGCCTAAATTGC	pES20
	rev	GCAATTTAGGCTCAAT**G**CGAACGGAGTGCCGTATC	
FgaPT2_K174E	fw	CTATCAGGACGCAGAAC**G**AGCTCGCGCTCGATC	pES23
	rev	GATCGAGCGCGAGCT**C**GTTCTGCGTCCTGATAG	
FgaPT2_K174Q	fw	CTATCAGGACGCAGAAC**C**AGCTCGCGCTCGATC	pES24
	rev	GATCGAGCGCGAGCT**G**GTTCTGCGTCCTGATAG	
FgaPT2_I80F	fw	CCCGCTGGTTGAGC**T**TCCTCACTCGATACGGC	pES25
	rev	GCCGTATCGAGTGAGG**AA**GCTCAACCAGCGGG	
FgaPT2_K174F	fw	CTATCAGGACGCAGAAC**TTC**CTCGCGCTCGATCTG	pES26
	rev	CAGATCGAGCGCGAG**GAA**GTTCTGCGTCCTGATAG	
FgaPT2_R244E	2fw	GCCAGTCCC**GAG**CTAGTGTCCTGTGATCTGACCAGTCC	pALF28
	2rev	GGACACTAG**CTC**GGGACTGGCAGTGCTCTTGGAACCGC	
FgaPT2_T102V	fw	GTGAGATAC**GT**ATTCGAGCCGATCAAT	pALF22
	rev	CGGCTCGAATA**C**GTATCTCACTATTGA	
FgaPT2_T102G	fw	GTGAGATAC**SGC**TTCGAGCCGATCAAT	pALF13
FgaPT2_T102C			pALF15
FgaPT2_T102S	rev	CGGCTCGAA**GCW**GTATCTCACTATTGA	pALF16
FgaPT2_T102R			pALF18
FgaPT2_K174W	fw	ACGCAGAAC**TG**GCTCGCGCTCGATCTG	pALF26
	rev	GAGCGCGAGC**CA**GTTCTGCGTCCTGAT	
FgaPT2_K174Y	fw	ACGCAGAAC**TAT**CTCGCGCTCGATCTG	pALF27
	rev	GAGCGCGAG**ATA**GTTCTGCGTCCTGAT	
FgaPT2_R244D	fw	GCCAGTCCC**RAT**CTAGTGTCCTGTGAT	pALF23
FgaPT2_R244N	rev	GGACACTAG**ATY**GGGACTGGCAGTGCT	pALF24
FgaPT2_R244Q	fw	GCCAGTCCCC**AA**CTAGTGTCCTGTGAT	pALF25
	rev	GGACACTAG**TT**GGGGACTGGCAGTGCT	

EXPERIMENTAL PROCEDURES

Chemicals—DMAPP was synthesized according to the method described for geranyl diphosphate reported previously (32). Substrates used for the enzyme assays were purchased at the highest available purity.

Bacterial Strains, Plasmids, and Culture Conditions—*Escherichia coli* XL1 Blue MRF′ (Stratagene, Heidelberg, Germany) and *E. coli* BL21 (DE3)pLysS (Invitrogen, Karlsruhe, Germany) were used for cloning and expression experiments, respectively. pIU18 was used as construct for FgaPT2 overproduction as described previously (19) and as DNA template for site-directed mutagenesis experiments. *E. coli* cells harboring plasmids were grown in liquid Lysogeny Broth (LB) or Terrific Broth (TB) medium and on solid LB medium with 1.5% (w/v) agar at 37 °C. 25 μg ml^{-1} of kanamycin were used for selection of recombinant *E. coli* strains.

Site-directed Mutagenesis—One-step site-directed mutagenesis protocols were used to generate the mutated derivatives of FgaPT2 listed in Table 1. The QuikChange site-directed mutagenesis kit (Stratagene, Heidelberg, Germany) was used for construction of plasmids pES23 to pES26 and pES34, the Expand Long Template PCR dNTP pack (Roche Diagnostics, Mannheim, Germany) was used for plasmids pALF13, pALF15, pALF16, pALF18, and pALF22, and the Expand Long Template PCR system (Roche Diagnostic, Mannheim, Germany) was used for plasmids pALF23 to pALF28. pES26 was used as template for construction of the double mutant K174F_R244E in pES34 with the primers R244E 2fw and R244E 2rev (Table 1). The obtained plasmids were subjected to sequencing to confirm the desired mutations in the respective constructs.

Overproduction and Purification of the Recombinant Proteins—FgaPT2 and its mutated derivatives were overproduced and purified as described previously (19) and analyzed on SDS-PAGE (Fig. 2). Protein yields between 0.6 and 4.9 mg/liter of culture were obtained in this study.

Enzyme Assays with Recombinant Purified Proteins—To determine the enzyme activity, the incubation mixtures contained 50 mM Tris-HCl (pH 7.5), 5 mM $CaCl_2$, 1 mM aromatic substrate, 1 or 2 mM DMAPP, 0.15–5% (v/v) glycerol, 0–5% (v/v) dimethyl sulfoxide (DMSO), and 0.2–0.4 mg ml^{-1} of purified recombinant protein in a total volume of 100 μl. After incubation at 37 °C for 6 or 16 h, the reactions were terminated by the addition of 100 μl of methanol. Protein was removed by centrifugation at 13,000 rpm for 20 min, and the supernatant was analyzed on HPLC. Data given in this study were calculated from two or three independent measurements.

To determine the kinetic parameters of aromatic substrates, DMAPP at 1 mM and aromatic substrates with concentrations of up to 2 mM were used. Variable protein concentrations and incubation times were used for different enzymes.

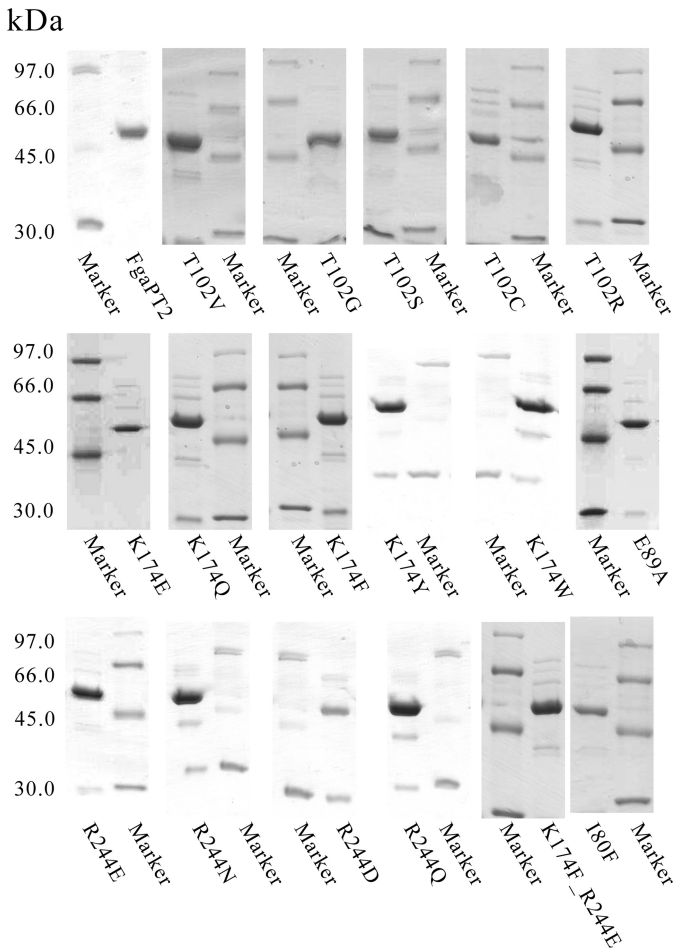

FIGURE 2. **Analysis of the overproduced and purified FgaPT2 and its 17 mutants on SDS-PAGE.** The purified proteins were separated, together with the low molecular weight calibration kit (GE Healthcare), on 12% SDS-polyacrylamide gels and stained with Coomassie Brilliant Blue G-250.

For isolation of the enzyme products, reactions were carried out in large scales (10 ml) containing 50 mM Tris-HCl (pH 7.5), 5 mM $CaCl_2$, 1 mM aromatic substrate, 1.5 mM DMAPP, and 0.2–0.4 mg ml^{-1} recombinant protein. After incubation at 37 °C for 16 h, the reactions were terminated by the addition of 10 ml of methanol. After removal of the precipitated protein by centrifugation at 6000 rpm for 30 min, the reaction mixtures were concentrated on a rotating vacuum evaporator at 35 °C to a final volume of 1 ml before injection into HPLC.

HPLC Analysis and Isolation of the Enzyme Products—The enzyme reaction mixtures were analyzed on HPLC (Agilent series 1200, Böblingen, Germany) by using a Multospher 120 RP-18 column (250 × 4 mm, 5 μm, CS-Chromatographie Service, Langerwehe, Germany) at a flow rate of 1 ml min^{-1}. Water (solvent A) and methanol (solvent B) were used as solvents. For analysis of the enzyme products, a linear gradient of 30–100% (v/v) solvent B in 20 min was used. The column was then washed with 100% (v/v) solvent B for 5 min and equilibrated with 30% (v/v) solvent B for 5 min. Detection was carried out with a photodiode array detector and illustrated at 277 nm in this study. For isolation of the enzyme products, the same HPLC equipment with a Multospher 120 RP-18 column (250 × 10 mm, 5 μm, CS-Chromatographie Service) was used. A linear gradient of 50–100% (v/v) of methanol (solvent B) in water (solvent A) in 50–80 min was carried out with a flow rate at 2.5 ml min^{-1}. The column was then washed with 100% (v/v) solvent B for 10 min and equilibrated with 50% (v/v) solvent B for 10 min.

TABLE 2
NMR data of the enzyme products in D_2O (500 MHz)
Chemical shifts (δ) are given in ppm, and coupling constants (J) are in Hz.

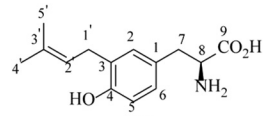

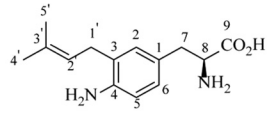

Pos.	δ_H, multi, J	δ_C	δ_H, multi, J	δ_C
1	-	127.3	-	126.4
2	7.15, d, 2.0	130.7	7.09, d, 1.6	130.3
3	-	128.9	-	128.2
4	-	152.8	-	143.3
5	6.92, d, 8.1	115.7	6.89, d, 8.1	117.3
6	7.08, dd, 8.1, 2.0	128.0	7.06, dd, 8.1, 1.6	128.0
7	3.23, dd, 14.8, 5.1 3.04, dd, 14.8, 8.1	35.4	3.21, dd, 14.5, 4.3 3.02, dd, 14.5, 8.0	35.9
8	3.95, dd, 8.1, 5.1	56.2	3.93, br s	56.2
9	-	174.0	-	174.7
1′	approx. 3.35[a]	27.8	3.30, d, 7.2	29.6
2′	5.41, tsept, 7.3, 1.4	121.9	5.34, tsept, 7.2, 1.4	120.9
3′	-	134.6	-	135.3
4′	1.78, s	16.9	1.81, s	17.0
5′	1.78, s	24.8	1.81, s	24.7

[a] Signals overlapping with those of methanol.

NMR and Mass Spectrometric Analyses—For structural elucidation, the isolated enzyme products were subjected to ^1H NMR, HSQC, HMBC, and MS analyses. High resolution electron impact mass spectrometry data were obtained on a Micromass Auto Spec spectrometer (Waters, Milford, MA). The enzyme products were: **1b**, m/z 249.1361 ($C_{14}H_{19}NO_3$, calculated, 249.1365); **3b**, m/z 248.1524 ($C_{14}H_{20}N_2O_2$, calculated, 248.1525).

For NMR analysis, the enzyme products were dissolved in CD_3OD or D_2O. Spectra were recorded at room temperature with an ECX-500 spectrometer (JEOL, Tokyo, Japan) equipped with a broadband probe with z-gradient. Chemical shifts were referenced to the solvent signal at 3.30 ppm for CD_3OD or 4.79 ppm for D_2O. All spectra were processed with MestReNova 5.2.2 (Mestrelab Research, Santiago de Compostela, Spain). NMR data of the isolated products are given in Table 2.

Molecular Docking Calculation—The structure of FgaPT2 (3I4X) in complex with tryptophan was used as a template for the docking calculation using AUTODOCK4 (33). The tryptophan and surrounding water molecules were removed, and the prenylation substrate, dimethylallyl *S*-thiolodiphosphate (DMSPP), was kept in the active site and assumed to be rigid. For docking calculations with L-tyrosine, Lys-174 was mutated to phenylalanine *in silico*. Docking calculations (genetic algorithm) were prepared with ADT (33) using a grid that covers the complete binding site. The results were visualized with PyMOL (48) and verified for chemical sense.

RESULTS

Acceptance of L-Tyrosine and 4-Amino-L-phenylalanine by FgaPT2—HPLC analysis of the incubation mixture of L-tryptophan with 0.36 μM FgaPT2 showed a conversion yield of 58 ±

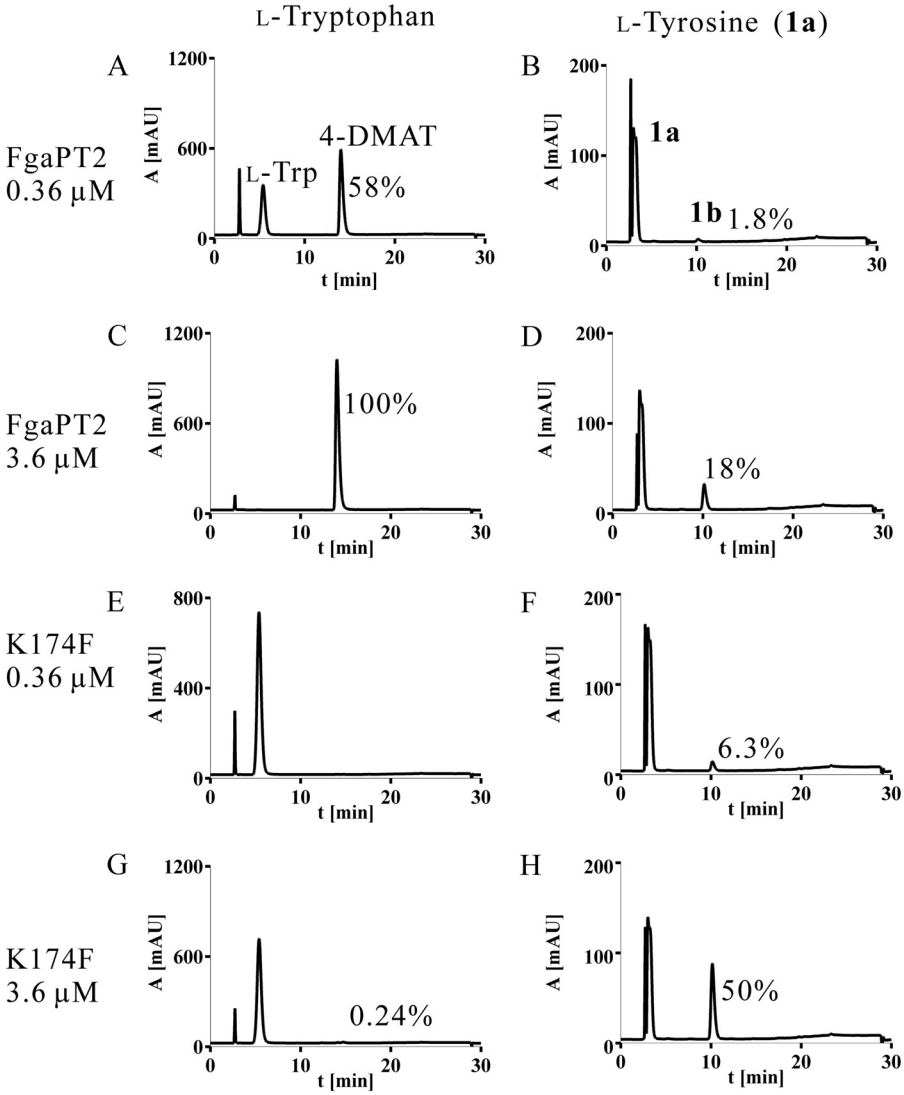

FIGURE 3. **HPLC analysis of incubation mixtures of L-tryptophan and L-tyrosine (1a) with FgaPT2 (*A–D*) and its mutant FgaPT2_K174F (*E–H*).** The enzyme assays contained 0.36 or 3.6 μM of the recombinant enzymes and were incubated at 37 °C for 16 h. Detection was carried out with a photodiode array detector and illustrated for absorption at 277 nm. *mAU*, milliabsorbance units.

1.0% (Fig. 3*A*). Using the same amount of protein, a minor additional peak with an approximate conversion of 1.8 ± 0.15% was detected in the incubation mixture of L-tyrosine (**1a**) (Fig. 3*B*). By increasing the FgaPT2 concentration to 3.6 μM, a clear and unique product peak with a yield of 18 ± 1.0% was observed in the HPLC chromatogram of **1a** (Fig. 3*D*). Under this condition, L-tryptophan was completely converted to 4-dimethylallyl tryptophan (4-DMAT) (Fig. 3*C*). No product formation was detected in the incubation mixtures of **1a** with 3.6 μM 5-DMATS or 6-DMATS$_{Sa}$ (data not shown). Interestingly, the retention time of the enzyme product of FgaPT2 with **1a** was found to be 10 min, which is 2 min shorter than that of the *O*-prenylated derivative obtained from the 7-DMATS assay under the same HPLC condition (data not shown) (30). This indicated the presence of different products in the reaction mixtures of **1a** with both tryptophan prenyltransferases. To test the substrate specificity of FgaPT2 toward tyrosine derivatives, D-tyrosine (**2a**), 4-amino-L-phenylalanine (**3a**), α-methyl-L-tyrosine (**4a**), 3-fluoro-DL-tyrosine (**5a**), 3-iodo-L-tyrosine (**6a**), 3-nitro-L-tyrosine (**7a**), 3,5-dibromo-L-tyrosine (**8a**), and 3,5-diiodo-L-tyrosine (**9a**) were incubated with 3.6 μM recombinant FgaPT2 at 37 °C for 16 h. As shown in Fig. 4, FgaPT2 showed a relatively high substrate specificity toward L-tyrosine and its analogue **3a**. Clear product formation was only observed in the reaction mixture of **3a** (data for **2a** and **4a**–**9a** not shown). With a total product yield of 70 ± 4.9%, **3a** was even better accepted by FgaPT2 than **1a**. Inspection of the HPLC chromatogram of the reaction mixture of **3a** revealed the presence of two product peaks **3b** and **3c** at 9.7 and 12 min, with product yields of 67 ± 4.5 and 3 ± 0.46%, respectively (Fig. 4*B*).

Enzyme Product Characterization—For structure elucidation, the enzyme products **1b**, **3b**, and **3c** were isolated from 10-ml enzyme reaction mixtures of **1a** and **3a**, respectively, and subjected to MS and NMR analyses. The obtained NMR data are given in Table 2. MS data indicated a monoprenylation in the isolated products **1b**, **3b**, and **3c** by detection of molecular masses, which are 68 Da larger than those of the respective substrates (see "Experimental Procedures"). The ^{1}H NMR spec-

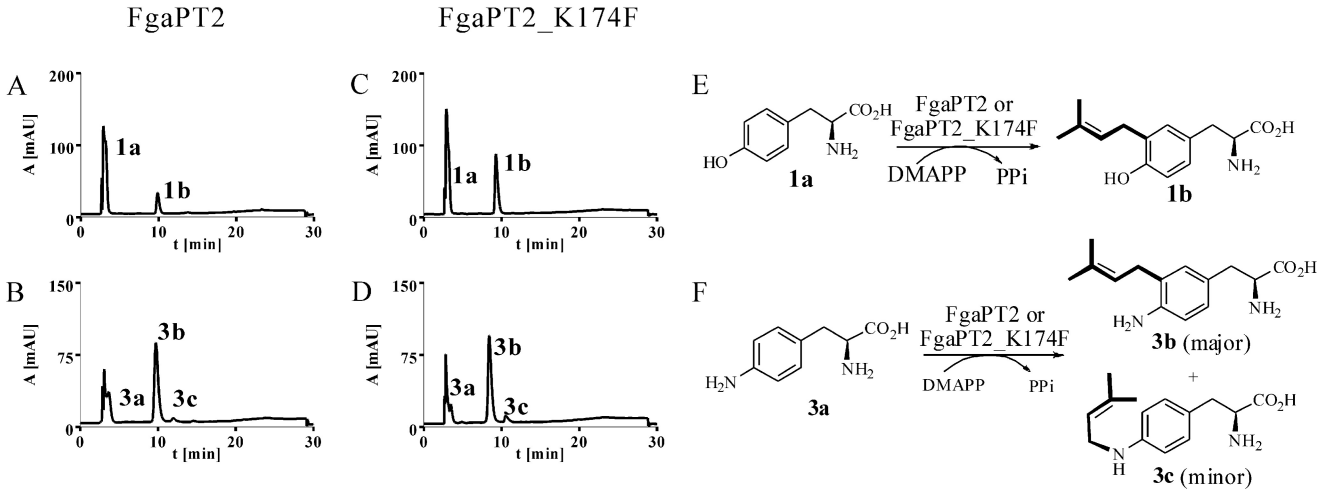

FIGURE 4. **HPLC analysis of the reaction mixtures of 1a (*A* and *C*) and 3a (*B* and *D*) with FgaPT2 or FgaPT2_K174F as well as prenyl transfer reactions catalyzed by both enzymes (*E* and *F*).** The enzyme assays contained 3.6 μM of the recombinant enzymes and were incubated at 37 °C for 16 h. Detection was carried out with a photodiode array detector and illustrated for absorption at 277 nm. *mAU*, milliabsorbance units.

trum of **3c** corresponded perfectly to that of the regularly *N*-prenylated derivative of **3a**, which had been identified as an enzyme product of SirD previously (28).

Inspection of the ^{1}H NMR spectra of **1b** and **3b** revealed the presence of only one product each. The signal of H-2′ at 5.41 ppm (triple septettes, 7.3, 1.4 Hz for **1b**) or 5.34 ppm (triple septettes, 7.2, 1.4 Hz for **3b**) proved them to be regularly prenylated products. Signals of three coupling aromatic protons were observed in spectra of both **1b** and **3b**, indicating the prenylation at an aromatic carbon atom of **1a** and **3a**. The coupling patterns of one doublet with a small coupling constant of 2.0 (**1a**) or 1.6 Hz (**3b**), one doublet with a large coupling constant of 8.1 Hz, and one double doublet with coupling constants of 8.1 and 2.0 Hz (**1b**) or 8.1 and 1.6 Hz (**3b**) also proved a C^2- or C^3-prenylation in **1b** and **3b** (Table 2). Given the electron donating effects of the 4-hydroxyl in **1a** or 4-amino group in **3a**, the Friedel-Crafts alkylation should take place at C-3 of the benzene ring. To prove this hypothesis, HSQC and HMBC spectra of **1b** and **3b** were then taken for structure determination. In the HSQC spectrum of **1b**, the chemical shifts of the three aromatic proton-bearing carbons are found at 130.7, 115.7, and 128.0 ppm, which were assigned to C-2, C-5, and C-6 of the C^3-prenylated product, respectively (Table 2). Clear HMBC correlations between H-1′ of the prenyl moiety and C-4 of the benzene ring as well as H-2 and C-1′ proved unequivocally that **1b** was the C^3-prenylated product. Furthermore, the ^{1}H NMR spectrum of **1b** taken in CD_3OD corresponded perfectly to that of the natural product isolated from *Streptomyces* sp. IFM 10937 (34). Similar correlations were observed in the HMBC spectrum of **3b**, and the same conclusion can be therefore drawn for this compound. These results confirmed the C^3-prenylation of **1a** and **3a** by FgaPT2 (Fig. 4, *E* and *F*) as the unique or main reaction (95.7%). In the case of **3a**, the *N*-prenylation was only 4.3% of the total product formation.

Molecular Modeling and Site-directed Mutagenesis of FgaPT2—To get more insights into the catalytic mechanism of FgaPT2 toward **1a** and **3a**, we carried out a molecular modeling study with FgaPT2 and **1a** based on the crystal ternary complex of FgaPT2 with DMSPP and L-tryptophan (21). We performed *in silico* docking of L-tyrosine (blue) into the binding pocket of L-tryptophan (Fig. 5). The final docking result is in good agreement with the observed catalytic activity and shows that the hydroxyl group occurs near a cavity occupied with water molecules (Fig. 5, *red spheres*). The C^3-atom of **1a** or **3a** (Fig. 5, *blue sphere*) can easily attack the C^1-atom of DMSPP. This model explained well our experimental results that **1a** and **3a** were also substrates for FgaPT2 and that the resulting products were C^3-prenylated derivatives.

According to this model, Thr-102 was proposed to interact with the hydroxyl group of **1a** or amino group of **3a** through hydrogen bond. Arg-244, Tyr-191, Leu-81, and Ile-80 tend to stabilize the side chain. Tyr-413, Lys-187, Arg-100, Tyr-409, Arg-404, Arg-257, Gln-343, and Lys-259 are involved in the diphosphate binding sites. In a previous study for the FgaPT2 reaction with L-tryptophan (21), Lys-174 was proposed to act as a base for abstracting the proton at C-4 from an intermediate, which was formed after attacking of C-4 to the prenyl cation, and rebuilding the aromatic ring. Later, Luk *et al.* (35) reported that the FgaPT2 reaction with tryptophan might undergo a reverse prenylation at C-3 followed by a Cope rearrangement and rearomatization. In both proposed mechanisms, Lys-174 always acted as a base for regaining the aromatic ring. The function as a base is lost for K174F at this position, which is accompanied by the prenylation of L-tyrosine at its C-3 atom. In our structural model, the carboxyl entity of Glu-89, which has an interaction with N-1 of L-tryptophan (21, 35), is oriented toward the C-3 of **1a** or **3a** and therefore suitable to function as a base to abstract the proton from the σ-complex.

To prove the proposed mechanism, we determined the activity of I80F, E89A, K174E, and K174Q obtained in a previous study (21) toward L-tryptophan and L-tyrosine by incubation at 37 °C for 6 h. As shown in Fig. 6, relative activities of 43.2 ± 2.0, 2.3 ± 0.21, 2.0 ± 0.24, and 119.0 ± 9.3% of that of FgaPT2 were detected for I80F, E89A, K174E, and K174Q with L-tryptophan, respectively. The results for I80F, E89A, and K174E are similar to those obtained in the previous study (21). Differing from that observed by Metzger *et al.* (21), K174Q showed a slightly higher activity than FgaPT2. This result indicated that Gln could elim-

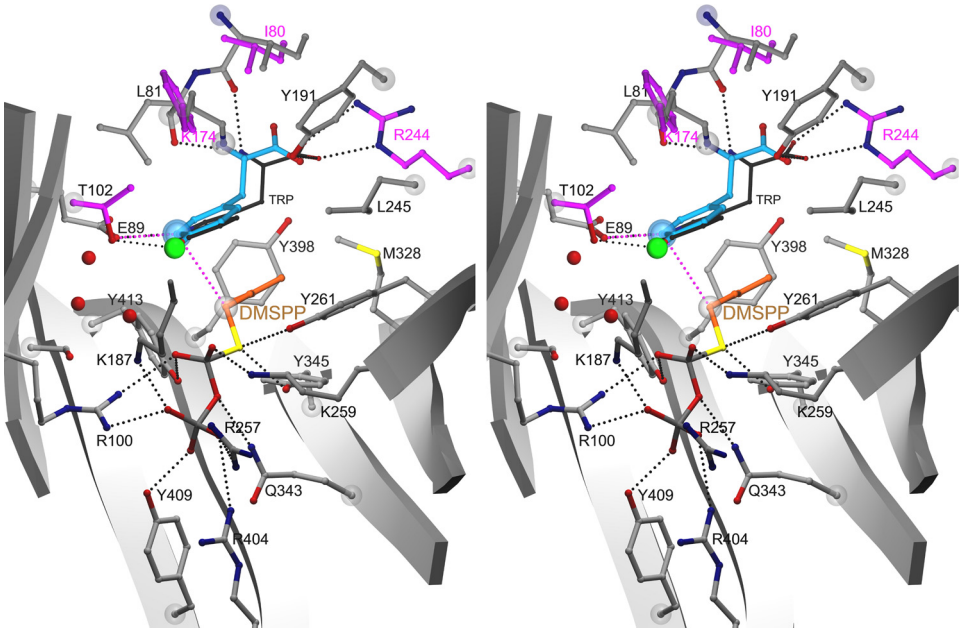

FIGURE 5. **The stereo view of active sites and proposed reaction model of FgaPT2 with 1a and 3a.** The active site of FgaPT2 is shown in a stick representation (*gray*). Three β-strands and Tyr-189 were removed to give a detailed view into the active site. The substrates **1a** and **3a** (*blue*; amino moiety or hydroxyl group is marked as a *green sphere*) are docked into the active site of FgaPT2_K174F using AUTODOCK4 and superimposed very well with the natural substrate tryptophan (*black*). This is possible because the binding site is designed to be occupied by a larger tryptophan residue. The hydroxyl or amino group of **1a** and **3a**, respectively, occurs near a cavity occupied with water molecules (*red spheres*). The C^3-atom of L-tyrosine (*blue sphere*) can easily attack the C^1-atom of DMSPP (*pink dotted lines*). Amino acids that were mutated in our experiments are colored in *magenta*.

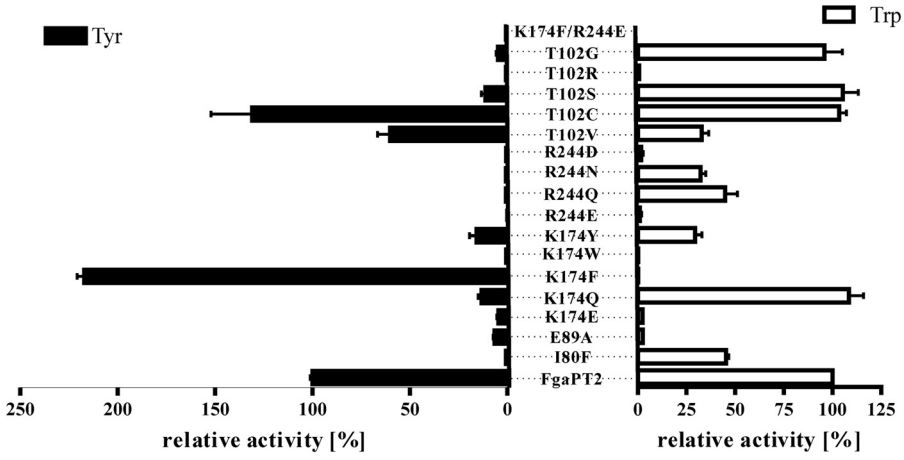

FIGURE 6. **Relative activities of FgaPT2 and its mutants with L-tryptophan or L-tyrosine as aromatic substrate.** The assays with L-tryptophan and L-tyrosine contained 0.36 and 3.6 μM recombinant proteins, respectively, and were incubated at 37 °C for 6 h. The absolute product yield of FgaPT2 with L-tryptophan (42 ± 2.0%) was defined as 100% relative activity. For L-tyrosine with FgaPT2, this value was 19 ± 1.6%. *Error bars* represent S.D. from three independent measurements.

inate a proton, or that another amino acid acts as a base instead. Using L-tyrosine as prenyl acceptor, relative activities of 0.62 ± 0.05, 5.7 ± 1.0, 3.2 ± 0.26, and 9.8 ± 0.89% of that of FgaPT2 were detected for I80F, E89A, K174E, and K174Q, respectively. This indicated different behaviors of I80F and K174Q toward L-tryptophan and L-tyrosine and suggested that Lys-174 was important but not the base to abstract a proton. Meanwhile, the significant activity decrease of E89A implied that it could be the base and supported our molecular model for the FgaPT2 reaction with L-tyrosine.

For further investigation, we chose three amino acids residues, Thr-102, Lys-174, and Arg-244 in the structure of FgaPT2 as "hot spots" for site-directed mutagenesis using primers listed in Table 1. We speculated that replacement of Lys-174 by an aromatic amino acid residue would have more interaction with the benzene ring of the substrate L-tyrosine and stabilize the intermediates of the prenylation. Therefore, we prepared additional Lys-174 mutants FgaPT2_K174F, FgaPT2_K174Y, and FgaPT2_K174W.

In another previous study, we showed that the cyclic dipeptide brevianamide F prenyltransferase FtmPT1 from *A. fumigatus* shared a similar structure and reaction chamber with FgaPT2 (36). However, the amino acid residues involved in the substrate binding differ slightly from each other. For example, Gly-115 in FtmPT1 was proposed to be involved in the binding of brevianamide F (36). The corresponding Thr-102 in FgaPT2

is likely not directly involved in the binding of L-tryptophan, but located in the active site of the enzyme (21). Mutation of Gly-115 in FtmPT1 to threonine resulted in a derivative, which catalyzed a reverse C^3- instead of a regular C^2-prenylation of brevianamide F (36). As shown in Fig. 5, Thr-102 in FgaPT2 is suggested to be involved in the binding of L-tyrosine. Therefore, we changed this residue to five different amino acids to get FgaPT2_T102*X* (*X* = Val, Arg, Cys, Gly, or Ser). In addition, molecular modeling indicated the binding of the amino group of the L-tyrosine side chain to Arg-244. Thus, different mutants at this position, FgaPT2_R244*X* (*X* = Glu, Asn, Asp, or Gln), were constructed as described under "Experimental Procedures." In total, we designed 13 additional mutants (Table 1) on the basis of the proposed mechanism as well as physical and chemical properties of the amino acids for investigation on enzyme activities.

Identification of the FgaPT2 Mutant Carrying Tyrosine C^3-Prenyltransferase but Almost No Tryptophan Prenyltransferase Activity—To evaluate the activity of the resulting mutants, the constructs obtained from site-directed mutagenesis experiments were introduced into *E. coli* BL21 (DE3)pLysS cells. After induction of the gene expression as described previously (19), the overproduced proteins were purified on nickel-nitrilotriacetic acid-agarose and used for enzyme assays with L-tryptophan or L-tyrosine under the same condition for FgaPT2 mentioned above (37 °C for 6 h). The obtained results for all of the 17 mutants with L-tryptophan and L-tyrosine are illustrated in Fig. 6 and compared with those of FgaPT2.

As shown in Figs. 3 and 6, clearly different activity profiles were observed for these mutants toward L-tryptophan and L-tyrosine. Similar or slightly higher, but in most cases, lower activity than that of non-mutated FgaPT2 was detected in the incubation mixtures of L-tryptophan with 0.36 μM recombinant mutants. Using L-tyrosine as substrate, most mutants showed much lower activities than FgaPT2. No significant changes on the activities were detected for T102C with L-tryptophan and L-tyrosine. Substantial increase of the enzyme activity toward L-tyrosine was detected for K174F. Approximate 3-fold activity of that of FgaPT2 was calculated for this mutant (Fig. 3). On the other hand, no conversion was detected in the incubation mixture of L-tryptophan with 0.36 μM K174F, even after an incubation for 16 h (Fig. 3*E*). Increasing the protein concentration to 3.6 μM and incubation time to 16 h, a minor product peak with a yield of 0.24 ± 0.073% was detected for K174F (Fig. 3*G*). With this protein concentration, a product yield of 50 ± 3.5% was calculated for K174F with **1a** as substrate (Fig. 3*H*). Isolation and structure elucidation confirmed the same enzyme product as that identified from the incubation mixture of FgaPT2 with **1a**. From these results, it can be concluded that K174F functions as a tyrosine C^3-prenyltransferase and not as tryptophan prenyltransferase anymore. K174F in a concentration of 3.6 μM was then incubated with eight tyrosine derivatives **2a–9a** at 37 °C for 16 h. The product yield of **3a** with K174F was slightly increased to 76 ± 4.4% (Fig. 4). No product formation was detected in the incubation mixtures of other substrates (data not shown).

Determination of Kinetic Parameters for FgaPT2 and Its Mutant by Using L-Tyrosine as Substrate—To compare the catalytic efficiencies of FgaPT2 and FgaPT2_K174F toward **1a**, kinetic parameters were determined by Eadie-Hofstee, Hanes-Woolf, and Lineweaver-Burk plots as described under "Experimental Procedures." K_m value of 0.58 ± 0.0082 mM was found for K174F, significantly lower than that of FgaPT2 at 0.82 ± 0.070 mM. The turnover number of K174F toward **1a** at 0.010 ± 0.000049 s^{-1} was 3.4-fold of that of FgaPT2 at 0.0029 ± 0.000034 s^{-1}. As consequence, the catalytic efficiency (k_{cat}/K_m) of K174F with **1a** as substrate was improved to 4.9-fold, in comparison with the non-mutated FgaPT2.

DISCUSSION

Prenylated aromatic compounds represent a large group of secondary metabolites and are widely distributed in bacteria, fungi, and plants (1, 3, 5, 37). In comparison with their non-prenylated precursors, these compounds show distinct and in general more potent biological and pharmacological activities (2, 3, 38, 39). Prenylated tyrosine and derivatives build a small group within the prenylated aromatic natural products (40, 41). 3-Dimethylallyl-L-tyrosine was isolated from *Streptomyces* sp. IFM 10937 in 2008 during a screening program for TNF-related apoptosis-inducing ligand (TRAIL) resistance-overcoming activity, together with *N*-acetyl-3-prenyl-L-tyrosine (34). However, neither the biosynthetic pathway of this type of natural products nor an enzyme for L-tyrosine C^3-prenylation has been reported until now.

Prenyltransferases represent key enzymes in the biosynthesis of prenylated natural products (1, 3, 4, 8, 42). Because of genome sequencing and mining of biosynthetic pathways, significant progress has been achieved on the genetics, enzymology, and structure of prenyltransferases using various aromatic substrates such as indoles including tryptophan, flavonoids, coumarins, xanthones, and naphthalenes (1, 3, 4, 8, 43). A number of studies have demonstrated the high flexibility of prenyltransferases, especially the members of the DMATS superfamily, toward their aromatic substrates (8). However, a switching of substrate preference by structure-based rational engineering has not been reported prior to this study.

Based on the fact that the L-tyrosine *O*-prenyltransferases SirD and TyrPT catalyzed C^7-prenylation of L-tryptophan and the tryptophan C^7-prenyltransferase 7-DMATS catalyzed the *O*-prenylation of L-tyrosine (14, 28, 30), we detected in this study the prenylation of L-tyrosine by the tryptophan C^4-prenyltransferase FgaPT2. Identification of enzyme product revealed a C^3-prenylation of L-tyrosine by FgaPT2, demonstrating the first enzymatic Friedel-Crafts alkylation of L-tyrosine as free amino acid. Subsequent molecular modeling-guided site-directed mutagenesis led to create an enzyme derivative K174F, which showed practically no activity toward L-tryptophan, whereas the acceptance of L-tyrosine by this enzyme was improved significantly. With 3.6 μM enzyme, a product yield of 50 ± 3.5% was detected for K174F after incubation at 37 °C for 16 h. Therefore, FgaPT2 and especially its mutant K174F represent the first series of L-tyrosine *C*-prenylating enzymes. Meanwhile, this study demonstrated the possibility to change

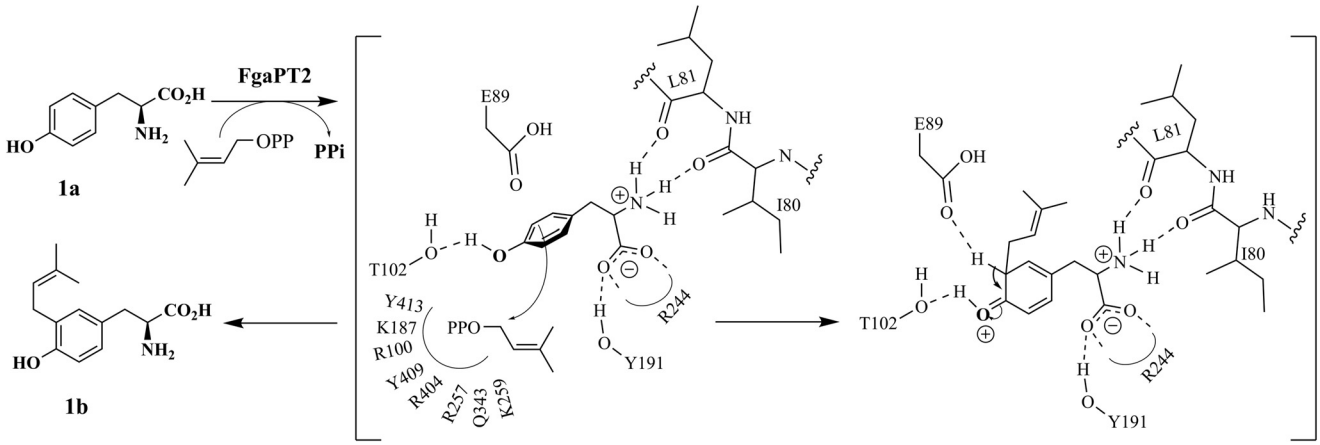

FIGURE 7. **Proposed mechanism for the conversion of 1a by FgaPT2 to the C^3-prenylated product 1b.** Interactions between the substrates and FgaPT2 were shown with *dotted lines*. The *curved arrows* show the direction of electron flow.

the substrate preference of a prenyltransferase by site-directed mutagenesis.

C-Prenylated tyrosyl residue was found in cyclic peptides, *e.g.* cyanobactins, from cyanobacteria (40, 44). A prenyltransferase *LynF in Lyngbya aestuarii* from the TruF enzyme family was proven to catalyze reverse *O*-prenylations of tyrosyl residues in such ribosomal cyclic peptides. *C*-Prenylated tyrosine-containing derivatives are then formed from the *O*-prenylated tyrosyl residue by Claisen rearrangement afterward (44, 45). To exclude the possibility that the C^3-prenylated products **1b** and **3b** are rearrangement rather than enzyme products during the incubation procedure, we carried out incubations with **1a** and **3a** for 10, 15, 30, 60, 120, and 960 min. Similar profiles of the HPLC chromatograms were observed for different incubation times (data not shown). In the incubation mixtures of **1a**, only the product peak **1b** was detected. In the incubation mixtures of **3a**, the ratio of the peak area of **3b** to that of **3c** remained almost constant after different incubation times (approximately 22 ± 0.65:1). It seems that **3b** and **3c** are independently formed during the incubation. To provide more details on stability of **3b** and **3c**, **3a** was incubated with FgaPT2 at 37 °C for 2 h. The reaction mixture was then heated to 80 °C and maintained for 3 h. No change was observed for the ratio of **3b** and **3c** in the HPLC chromatogram of the treated sample, excluding the heat-catalyzed rearrangement between **3b** and **3c**.

Taking the results obtained from molecular modeling and mutagenesis experiments into consideration (Figs. 5 and 6), a mechanism was proposed for FgaPT2 reaction with **1a**. According to this hypothesis, the residue Thr-102 in FgaPT2 interacts with the 4-hydroxyl group of **1a** in the reaction cavity and contributes to the stabilization of the intermediate. A number of basic amino acids and tyrosine residues mentioned before are involved in the binding of DMAPP and responsible for the formation of the dimethylallyl carbon cation (21, 46). A detailed course of the reaction remained to be elucidated and might start by a nucleophilic attack of electron-rich C-3 of the benzene ring onto C-1′of the dimethylallyl carbon cation, resulting in the formation of an intermediate with a non-aromatic system. A plausible deprotonation to regain aromaticity might involve Glu-89 of FgaPT2, resulting in the formation of C^3-prenylated product **1b** (Fig. 7). In comparison with that of FgaPT2, FgaPT2_E89A showed only a relative activity of 5.7 ± 1.0% toward L-tyrosine, providing strong support for this hypothesis. It is also considerable that a reverse prenylation at C-1 is followed by a Cope rearrangement as proposed for FgaPT2 with L-tryptophan (35).

Using the molecular model mentioned above, the activities of other mutants obtained in this study can also be interpreted. For the mutation at Thr-102, substitution of Thr with similar amino acids, such as Cys and Ser, (partly) retained the catalytic ability toward L-tryptophan, whereas T102C demonstrated similar catalytic ability toward **1a** as FgaPT2, 1.9-fold of that of T102V, and 7.1-fold of that of T102S. This indicates that both the hydrogen donor and the methyl group are important for the activity of FgaPT2 toward **1a**. Although the hydrogen bond is not crucial for the reaction (T102V), steric collisions (T102R) abolish the reaction, whereas smaller side chains avoid the correct positioning of the aromatic ring systems (T102G). Interestingly, mutant T102C slightly increases the catalytic turnover as the nucleophilic sulfur atom is more suitable to stabilize the partial positive charge of the cationic intermediate.

By substitution of Lys-174 with Glu, Tyr, or Trp, the activities toward both L-tryptophan and **1a** were reduced or abolished, whereas K174F demonstrated a specific and 4.9-fold catalytic efficiency toward **1a**, but almost complete loss of activity toward L-tryptophan. The rigidity and increased size of the phenyl side chain of K174F seem to support the stabilization of a smaller substrate (tyrosine) in a cavity that was designed to incorporate a larger educt (tryptophan). Besides, the introduction of the mutation K174F is likely to induce minor conformational rearrangements to its neighboring residues of the indole binding site by steric restrains. The higher activity of K174F for **1a** could be interpreted by much better interaction of the modified cavity to the phenyl moiety with the benzene ring of L-tyrosine compared with the interaction with the indole ring of L-tryptophan.

All four mutated derivatives at Arg-244 showed poor conversion of L-tryptophan. Although FgaPT2 does accept the removal of the positive charge by the Arg-244 head group (R224Q and R244N), the introduction of a negative charge by R244E would abolish the prenylation of tryptophan due to charge-charge repulsion. The enzyme activities of these four

Arg-244 mutants toward L-tyrosine were abolished completely (Fig. 6), demonstrating its essential role in the interaction of FgaPT2 with the side chain of L-tyrosine. The absolute importance of this amino acid residue was also demonstrated by the double mutant K174F_R244E.

In this study, we reported the C^3-prenylation of L-tyrosine and 4-amino-L-phenylalanine by the tryptophan C^4-prenyltransferase FgaPT2 from the fungus *A. fumigatus* and demonstrated, to the best of our knowledge, the first enzymatic Friedel-Crafts alkylation of tyrosine and derivative as free amino acids. Our results provided additional evidence for the relationships of substrate and catalytic promiscuity between tryptophan and tyrosine prenyltransferases. Furthermore, a binding site different from that of L-tryptophan was proposed for L-tyrosine and used as the basis for rational design of FgaPT2 mutants. K174F exhibited much higher catalytic efficiency toward L-tyrosine than FgaPT2, whereas its activity toward L-tryptophan was almost abolished. C^3-Prenylated L-tyrosine and 4-amino-L-phenylalanine remained unique or predominant product of the mutant. The ratio of the product yields of L-tyrosine to L-tryptophan was increased from 1:31 with FgaPT2 to 208:1 with K174F. This means that K174F does not function as tryptophan prenyltransferase anymore. Moreover, it acts as L-tyrosine C^3-prenyltransferase and could serve as new biocatalyst for C^3-prenylation of L-tyrosine. Therefore, the result provides an exciting example for creating biocatalysts by mutation of known enzymes. It is also considerable that enzymes for specific prenylation of flavonoids or hydroxynaphthalenes could be created by mutation of some members of the DMATS superfamily because such compounds have already been accepted by some of these enzymes as prenylation substrates (20, 47). Meanwhile, this study presents an excellent example of successful interdisciplinary cooperation and of the importance of structure biology in the discovery and development of novel biocatalysts.

Acknowledgments—We thank Lena Ludwig for synthesis of DMAPP and Nina Zitzer and Stefan Newel for taking MS and NMR spectra, respectively.

REFERENCES

1. Heide, L. (2009) Prenyl transfer to aromatic substrates: genetics and enzymology. *Curr. Opin. Chem. Biol.* **13,** 171–179
2. Wollinsky, B., Ludwig, L., Hamacher, A., Yu, X., Kassack, M. U., and Li, S.-M. (2012) Prenylation at the indole ring leads to a significant increase of cytotoxicity of tryptophan-containing cyclic dipeptides. *Bioorg. Med. Chem. Lett.* **22,** 3866–3869
3. Li, S.-M. (2010) Prenylated indole derivatives from fungi: structure diversity, biological activities, biosynthesis and chemoenzymatic synthesis. *Nat. Prod. Rep.* **27,** 57–78
4. Yazaki, K., Sasaki, K., and Tsurumaru, Y. (2009) Prenylation of aromatic compounds, a key diversification of plant secondary metabolites. *Phytochemistry* **70,** 1739–1745
5. Botta, B., Vitali, A., Menendez, P., Misiti, D., and Delle Monache, G. (2005) Prenylated flavonoids: pharmacology and biotechnology. *Curr. Med. Chem.* **12,** 717–739
6. Lindel, T., Marsch, N., and Adla, S. K. (2012) Indole prenylation in alkaloid synthesis. *Top. Curr. Chem.* **309,** 67–129
7. Wessjohann, L. A., Keim, J., Weigel, B., and Dippe, M. (2013) Alkylating enzymes. *Curr. Opin. Chem. Biol.* **17,** 229–235
8. Yu, X., and Li, S.-M. (2012) Prenyltransferases of the dimethylallyltryptophan synthase superfamily. *Methods Enzymol.* **516,** 259–278
9. Li, S.-M. (2009) Applications of dimethylallyltryptophan synthases and other indole prenyltransferases for structural modification of natural products. *Appl. Microbiol. Biotechnol.* **84,** 631–639
10. Bonitz, T., Alva, V., Saleh, O., Lupas, A. N., and Heide, L. (2011) Evolutionary relationships of microbial aromatic prenyltransferases. *PLoS One* **6,** e27336
11. Winkelblech, J., and Li, S.-M. (2014) Biochemical investigations of two 6-DMATS enzymes from *Streptomyces* revealing novel features of L-tryptophan prenyltransferases. *Chembiochem.* **15,** 1030–1039
12. Pockrandt, D., Sack, C., Kosiol, T., and Li, S.-M. (2014) A promiscuous prenyltransferase from *Aspergillus oryzae* catalyses C-prenylations of hydroxynaphthalenes in the presence of different prenyl donors. *Appl. Microbiol. Biotechnol.* **98,** 4987–4994
13. Tarcz, S., Ludwig, L., and Li, S.-M. (2014) AstPT catalyses both reverse N^1- and regular C^2-prenylation of a methylated bisindolyl benzoquinone. *Chembiochem.* **15,** 108–116
14. Fan, A., Chen, H., Wu, R., Xu, H., and Li, S.-M. (2014) A new member of the DMATS superfamily from *Aspergillus niger* catalyzes prenylations of both tyrosine and tryptophan derivatives. *Appl. Microbiol. Biotechnol.* **98,** 10119–10129
15. Unsöld, I. A., and Li, S.-M. (2005) Overproduction, purification and characterization of FgaPT2, a dimethylallyltryptophan synthase from *Aspergillus fumigatus*. *Microbiology* **151,** 1499–1505
16. Wallwey, C., and Li, S.-M. (2011) Ergot alkaloids: structure diversity, biosynthetic gene clusters and functional proof of biosynthetic genes. *Nat. Prod. Rep.* **28,** 496–510
17. Liebhold, M., Xie, X., and Li, S.-M. (2012) Expansion of enzymatic Friedel-Crafts alkylation on indoles: acceptance of unnatural β-unsaturated allyl diphospates by dimethylallyl-tryptophan synthases. *Org. Lett.* **14,** 4882–4885
18. Liebhold, M., and Li, S.-M. (2013) Regiospecific benzylation of tryptophan and derivatives catalyzed by a fungal dimethylallyl transferase. *Org. Lett.* **15,** 5834–5837
19. Steffan, N., Unsöld, I. A., and Li, S.-M. (2007) Chemoenzymatic synthesis of prenylated indole derivatives by using a 4-dimethylallyltryptophan synthase from *Aspergillus fumigatus*. *Chembiochem* **8,** 1298–1307
20. Yu, X., Xie, X., and Li, S.-M. (2011) Substrate promiscuity of secondary metabolite enzymes: prenylation of hydroxynaphthalenes by fungal indole prenyltransferases. *Appl. Microbiol. Biotechnol.* **92,** 737–748
21. Metzger, U., Schall, C., Zocher, G., Unsöld, I., Stec, E., Li, S.-M., Heide, L., and Stehle, T. (2009) The structure of dimethylallyl tryptophan synthase reveals a common architecture of aromatic prenyltransferases in fungi and bacteria. *Proc. Natl. Acad. Sci. U.S.A.* **106,** 14309–14314
22. Luk, L. Y. P., and Tanner, M. E. (2009) Mechanism of dimethylallyltryptophan synthase: evidence for a dimethylallyl cation intermediate in an aromatic prenyltransferase reaction. *J. Am. Chem. Soc.* **131,** 13932–13933
23. Kremer, A., Westrich, L., and Li, S.-M. (2007) A 7-dimethylallyltryptophan synthase from *Aspergillus fumigatus*: overproduction, purification and biochemical characterization. *Microbiology* **153,** 3409–3416
24. Yin, W.-B., Baccile, J. A., Bok, J. W., Chen, Y., Keller, N. P., and Schroeder, F. C. (2013) A nonribosomal peptide synthetase-derived iron(III) complex from the pathogenic fungus *Aspergillus fumigatus*. *J. Am. Chem. Soc.* **135,** 2064–2067
25. Pockrandt, D., Ludwig, L., Fan, A., König, G. M., and Li, S.-M. (2012) New insights into the biosynthesis of prenylated xanthones: XptB from *Aspergillus nidulans* catalyses an *O*-prenylation of xanthones. *Chembiochem* **13,** 2764–2771
26. Kremer, A., and Li, S.-M. (2010) A tyrosine *O*-prenyltransferase catalyses the first pathway-specific step in the biosynthesis of sirodesmin PL. *Microbiology* **156,** 278–286
27. Gardiner, D. M., Cozijnsen, A. J., Wilson, L. M., Pedras, M. S., and Howlett, B. J. (2004) The sirodesmin biosynthetic gene cluster of the plant pathogenic fungus *Leptosphaeria maculans*. *Mol. Microbiol.* **53,** 1307–1318
28. Zou, H.-X., Xie, X., Zheng, X.-D., and Li, S.-M. (2011) The tyrosine *O*-prenyltransferase SirD catalyzes *O*-, *N*-, and *C*-prenylations. *Appl. Micro-*

biol. Biotechnol. **89,** 1443–1451
29. Rudolf, J. D., and Poulter, C. D. (2013) Tyrosine *O*-prenyltransferase SirD catalyzes *S*-, *C*-, and *N*-prenylations on tyrosine and tryptophan derivatives. *ACS Chemical Biology* **8,** 2707–2714
30. Fan, A., and Li, S.-M. (2014) Prenylation of tyrosine and derivatives by a tryptophan C^7-prenyltransferase. *Tetrahedron Lett.* **55,** 5199–5202
31. Yu, X., Liu, Y., Xie, X., Zheng, X.-D., and Li, S.-M. (2012) Biochemical characterization of indole prenyltransferases: filling the last gap of prenylation positions by a 5-dimethylallyltryptophan synthase from *Aspergillus clavatus*. *J. Biol. Chem.* **287,** 1371–1380
32. Woodside, A. B., Huang, Z., and Poulter, C. D. (1988) Trisammonium geranyl diphosphate. *Org. Synth.* **66,** 211–215
33. Morris, G. M., Huey, R., Lindstrom, W., Sanner, M. F., Belew, R. K., Goodsell, D. S., and Olson, A. J. (2009) AutoDock4 and AutoDockTools4: automated docking with selective receptor flexibility. *J. Comput. Chem.* **30,** 2785–2791
34. Ahmed, F., Ohtsuki, T., Aida, W., and Ishibashi, M. (2008) Tyrosine derivatives isolated from *Streptomyces* sp. IFM 10937 in a screening program for TRAIL-resistance-overcoming activity. *J. Nat. Prod.* **71,** 1963–1966
35. Luk, L. Y., Qian, Q., and Tanner, M. E. (2011) A cope rearrangement in the reaction catalyzed by dimethylallyltryptophan synthase? *J. Am. Chem. Soc.* **133,** 12342–12345
36. Jost, M., Zocher, G., Tarcz, S., Matuschek, M., Xie, X., Li, S.-M., and Stehle, T. (2010) Structure-function analysis of an enzymatic prenyl transfer reaction identifies a reaction chamber with modifiable specificity. *J. Am. Chem. Soc.* **132,** 17849–17858
37. El-Seedi, H. R., El-Ghorab, D. M. H., El-Barbary, M. A., Zayed, M. F., Göransson, U., Larsson, S., and Verpoorte, R. (2009) Naturally occurring xanthones; latest investigations: isolation, structure elucidation and chemosystematic significance. *Curr. Med. Chem.* **16,** 2581–2626
38. Williams, R. M., Stocking, E. M., and Sanz-Cervera, J. F. (2000) Biosynthesis of prenylated alkaloids derived from tryptophan. *Top. Curr. Chem.* **209,** 97–173
39. Jain, H. D., Zhang, C., Zhou, S., Zhou, H., Ma, J., Liu, X., Liao, X., Deveau, A. M., Dieckhaus, C. M., Johnson, M. A., Smith, K. S., Macdonald, T. L., Kakeya, H., Osada, H., and Cook, J. M. (2008) Synthesis and structure-activity relationship studies on tryprostatin A, a potent inhibitor of breast cancer resistance protein. *Bioorg. Med. Chem.* **16,** 4626–4651
40. McIntosh, J. A., Lin, Z., Tianero, M. D., and Schmidt, E. W. (2013) Aestuaramides, a natural library of cyanobactin cyclic peptides resulting from isoprene-derived Claisen rearrangements. *ACS Chem. Biol.* **8,** 877–883
41. McIntosh, J. A., Donia, M. S., and Schmidt, E. W. (2009) Ribosomal peptide natural products: bridging the ribosomal and nonribosomal worlds. *Nat. Prod. Rep.* **26,** 537–559
42. Lu, Y. P., Liu, H. G., and Liang, P. H. (2009) Different reaction mechanisms for *cis*- and *trans*-prenyltransferases. *Biochem. Biophys. Res. Commun.* **379,** 351–355
43. Karamat, F., Olry, A., Munakata, R., Koeduka, T., Sugiyama, A., Paris, C., Hehn, A., Bourgaud, F., and Yazaki, K. (2014) A coumarin-specific prenyltransferase catalyzes the crucial biosynthetic reaction for furanocoumarin formation in parsley. *Plant J.* **77,** 627–638
44. McIntosh, J. A., Donia, M. S., Nair, S. K., and Schmidt, E. W. (2011) Enzymatic basis of ribosomal peptide prenylation in cyanobacteria. *J. Am. Chem. Soc.* **133,** 13698–13705
45. Majmudar, J. D., and Gibbs, R. A. (2011) Pericyclic prenylation: peptide modification through a Claisen rearrangement. *Chembiochem.* **12,** 2723–2726
46. Stec, E., Steffan, N., Kremer, A., Zou, H., Zheng, X., and Li, S.-M. (2008) Two lysine residues are responsible for the enzymatic activities of indole prenyltransferases from fungi. *Chembiochem* **9,** 2055–2058
47. Yu, X., and Li, S.-M. (2011) Prenylation of flavonoids by using a dimethylallyltryptophan synthase 7-DMATS from *Aspergillus fumigatus*. *Chembiochem* **12,** 2280–2283
48. DeLano, W. L. (2010) *The PyMOL Molecular Graphics System*, version 1.5.0.4, Schrödinger, LLC, New York

Enzymology:

Site-directed Mutagenesis Switching a Dimethylallyl Tryptophan Synthase to a Specific Tyrosine C^3-Prenylating Enzyme

Aili Fan, Georg Zocher, Edyta Stec, Thilo Stehle and Shu-Ming Li

J. Biol. Chem. 2015, 290:1364-1373.
doi: 10.1074/jbc.M114.623413 originally published online December 4, 2014